$X = 25$ mm on the ramp, where the mean flow speed nearby the wall is zero. Figure 8 *c* and *d* shows the mean velocity distributions in the *U* (left) and *V* (right) components of the same region. It can be seen from the *U*-component velocity cloud chart that shear layer is gradually close to the ramp, and the recirculation region which is covered by shear layer decreases gradually. The distributions of the *V*-component velocity are a continuation of the oblique *V* in the separation region.

1. Wu MinWei and Martin, P. M., Analysis of shock motion in shock wave and turbulent boundary layer interaction using direct numerical simulation data. *J. Fluid Mech.*, 2008, **594**, 71–83.
2. Edwards, J. R. and Boles, J. A., Large eddy Reynolds-averaged Navier–Stokes simulation of a Mach 5 compression–corner interaction. *AIAA J.*, 2008, **46**, 977–991.
3. Dawson, D. M., Kawai, S. and Lele, S. K., Large-eddy simulation of a Mach 2.9 turbulent boundary layer over a 24° compression ramp. In 41st AIAA Fluid Dynamics Conference, Honolulu, Hawaii, AIAA 2011–3431, 27–30 June 2011.
4. Gramann, R. A. and Dolling, D. S., A preliminary study of the turbulent structures associated with unsteady separation shock motion in a Mach 5 compression ramp interaction. AIAA paper 1992–0744.
5. Ringuette, M. J., Bookey, P. and Wyckham, C., Experimental study of a Mach 3 compression ramp interaction at $Re_\theta = 2400$. *AIAA J.*, 2009, **47**, 373–385.
6. Chan, S. C., Clemens, N. T. and Dolling, D. S., Flowfield imaging of unsteady, separated compression ramp interaction. In 26th AIAA Fluid Dynamics Conference, San Diego, USA, AIAA 1995–2195, 19–22 June 1995.
7. Zheltovodov, A. A., Some advances in research of shock wave turbulent boundary layer interactions. In 44th AIAA Aerospace Sciences Meeting, Reno Nevada, AIAA 2006–0496, 9–12 January 2006.
8. Yi, S. H., He, L., Zhao, Y. X. and Tian, L. F., A flow control study of a supersonic mixing layer via NPLS. *Sci. China Ser. G-Phys. Mech. Astron.*, 2009, **52**, 2001–2006.
9. Zhao, Y. X., Yi, S. H. and Tian, L. F., Supersonic flow imaging via nanoparticles. *Sci. China Ser. E-Tech. Sci.*, 2009, **52**, 3640–3648.
10. He, L., Yi, S. H., Zhao, Y. X., Tian, L. F. and Chen, Z., Visualization of coherent structures in a supersonic flat-plate boundary layer. *Chin. Sci. Bull.*, 2011, **56**, 489–494.
11. Chen, Z., Yi, S. H., He, L., Tian, L. F. and Zhu, Y. Z., An experimental study on fine structures of supersonic laminar/turbulent flow over a backward-facing step based on NPLS. *Chin. Sci. Bull.*, 2012, **57**, 584–590.
12. Wu, Y., Yi, S. H., Chen, Z., Zhang, Q. H. and Gang, D. D., Experimental investigations on structures of supersonic laminar/turbulent flow over a compression ramp. *Acta Phys. Sin.*, 2013, **62**, 184702.
13. Zhu, Y. Z., Yi, S. H., He, L. and Tian, L. F., Instantaneous and time-averaged flow structures around a blunt double-cone with or without supersonic film cooling visualized via nano-tracer planar laser scattering. *Chin. Phys. B*, 2013, **22**, 014702.
14. Ringuette, M. J. and Smits, A. J., Wall-pressure measurements in a Mach 3 shock wave turbulent boundary layer interaction at a DNS-accessible Reynolds number. In 37th AIAA Fluid Dynamics Conference, Miami, FL, AIAA 2007–4113, 25–28 June 2007.
15. Bookey, P., Wyckham, C. and Smits, A. J., Experimental investigations of Mach 3 shock-wave turbulent boundary layer interactions. In 35th AIAA Fluid Dynamics Conference, Toronto, Ontario, Canada, AIAA 2005–4899, 6–9 June 2005.
16. Verma, S. B., Experimental study of flow unsteadiness in a Mach 9 compression ramp interaction using a laser schlieren system. *Meas. Sci. Technol.*, 2003, **14**, 989–997.
17. Zhao, Y. X., Yi, S. H. and He, L., The experimental study of interaction between shock wave and turbulence. *Chin. Sci. Bull.*, 2007, **52**, 1297–1301.
18. Verma, S. B., Manisankar, C. and Raju, C., Control of shock unsteadiness in shock boundary-layer interaction on a compression corner using mechanical vortex generators. *Shock Waves*, 2012, **22**, 327–339.

ACKNOWLEDGEMENT. This research is supported by the National Natural Science Foundation of China (Grant No. 11172326 and Grant No. 11302256).

Received 25 March 2014; revised accepted 23 September 2014

Prevalence of *Wheat dwarf India virus* in wheat in India

Jitendra Kumar[#], Jitesh Kumar[#], Shashank Singh, Vishnu Shukla, Sudhir P. Singh and Rakesh Tuli*

National Agri-Food Biotechnology Institute, Mohali 160 071, India

***Wheat dwarf India virus* (*WDIV*) is the first mastrevirus reported to have subgenomic molecules called satellites. To establish association of the satellites with *WDIV* across a variety of ecoclimatic conditions, a countrywide survey was carried out. *WDIV* and its associated satellites (alphasatellite and betasatellite) were identified in plant samples collected from each of the 14 field locations surveyed in the study. Though there were location- and variety-related differences in disease scale, most of the infected wheat cultivars in fields across the country carried both the satellites. The wide occurrence of *WDIV* disease complex in India suggests the need to assess how the spread of *WDIV* and its satellites can be limited in wheat fields.**

Keywords: Alphasatellite, atypical mastrevirus, betasatellite, symptom severity.

WHEAT *dwarf India virus* (*WDIV*) is a leafhopper (*Psammotettix* sp.; family Cicadellidae) transmitted mastrevirus (family Geminiviridae) that infects wheat in India[1]. Dwarfing or stunting is the typical symptom of *WDIV*, but yellowing of leaves is also associated with field infection, which may be due to other factors[2]. Two alphasatellites (Cotton leaf curl Multan alphasatellite and Guar leaf

*For correspondence. (e-mail: rakeshtuli@hotmail.com)
[#]Contributed equally to this work.

curl alphasatellite) and a betasatellite (Ageratum leaf curl betasatellite) have been reported as associated with *WDIV* in field-infected wheat plants that do not show any begomovirus[2]. The presence of *WDIV* and the absence of begomovirus indicated the association of the satellites with *WDIV*. This was ascertained by inoculating *WDIV* in wheat, with or without satellites and detecting them in systemically infected leaves. Wheat plants inoculated with *WDIV* and any of the satellites showed more severe stunting in comparison to those inoculated with *WDIV* alone, thus establishing the role of the satellites in *WDIV* infection of wheat[2]. In a subsequent study, the associated Ageratum leaf curl betasatellite was reported to act as pathogenicity determinant in the infection by *WDIV*[3].

Wheat dwarf virus (*WDV*), another member of the genus *Mastrevirus*, is a causal agent of dwarfing, mottling, yellowing or reddening in wheat across the globe[4]. *WDV* is a ubiquitous wheat virus and has become a serious pathogen of wheat in Europe, Asia and Africa[4–8]. In spite of the ubiquitous nature of *WDV*, no sequence suggesting the presence of *WDV* was identified in the symptomatic (stunted) wheat plants during our study. Except *WDIV*, no mastrevirus has been reported to be associated with satellites. More studies are desirable to find the association of satellites with other members of the genus *Mastrevirus* (for example *WDV*, *Maize streak virus*) and their role in pathogenesis.

The ubiquitous nature of *WDV* and the identification of *WDIV* associated with satellites in India, propelled us to explore if *WDIV* along with the satellites was ubiquitous in the field infections of wheat in the country. We surveyed a number of geographically and agroclimatically widely separated wheat fields across the country. The present study reports the results of sampling done at 14 locations across India. Varietal effect on the disease severity and the prevalence of *WDIV* and its associated satellites (alphasatellite and betasatellites) are also reported.

Samples were collected from wheat fields in different parts of the country during 2011–2013 (Figure 1). Fourteen geographically distinct locations were surveyed. Leaf samples were collected from plants showing the primary symptom, i.e. dwarfing, without or with additional phenotypes such as sterile spikes and yellowing of leaves. Pathogenicity on the basis of plant height and other symptoms was determined on 0–9 scale (Table 1). Plants at scales 8 and 9 contained sterile spikes with no grain formation. At scale 3, 4 and 6, in addition to dwarfing, fungal infection was noticed. A total of 1005 samples were analysed, comprising 963 symptomatic (scale 1–9) and 42 asymptomatic (scale 0) plants. The leaf samples were labelled by variety and disease scale, and stored at –80°C till analysis.

Amplification of *WDIV* and associated satellites was done in polymerase chain reaction (PCR) using specific primers – MF1_FOR/REV and MF2_FOR/REV (ref. 1). Primer pairs β01/04 for the betasatellite and 'nanofor'/'nanorev' for the alphasatellite were used[9]. The PCR products were cloned into pDRIVE vector (Qiagen GmbH, Germany) and then sequenced using automated sequencer (Applied Biosystem 3730xl DNA Analyser, USA).

Nucleotide sequence search was done using BlastN to retrieve homologous sequences from the database. These were analysed using pairwise global alignment (http://www.ebi.ac.uk/Tools/psa/emboss_needle/nucleotide.html).

For calculating prevalence, total number of plants was counted in an area of 10 sq. ft. Samples were collected from all the locations for studying the presence of *WDIV* and the satellites in the suspected plants. The prevalence was calculated on the basis of total samples in a unit area and the number of virus-positive samples identified in that area.

Out of the 963 symptomatic plants collected during the survey, 791 yielded an amplicon of ~2.8 kb using *WDIV*-specific primers (MF1_FOR/REV and MF2_FOR/REV), thus indicating the presence of the virus (Table 2). Out of the 42 asymptomatic plants taken as negative controls, two gave an amplicon of ~2.8 kb. The two plants at scale 0 belonged to cv Sonalika, which has been reported to show mild symptoms upon infection by *WDIV* and the satellites[2]. Sequencing of the fragment of ~2.8 kb established the presence of *WDIV* in all the PCR-positive samples. PCR amplification using the alphasatellite and betasatellite-specific primers ('nanofor'/'nanorev' and β01/04) yielded an amplicon of ~1.3 kb in the samples found positive for *WDIV*.

The viral genomes detected from the samples were 99.5–100% identical to *WDIV* (accession nos JF781306,

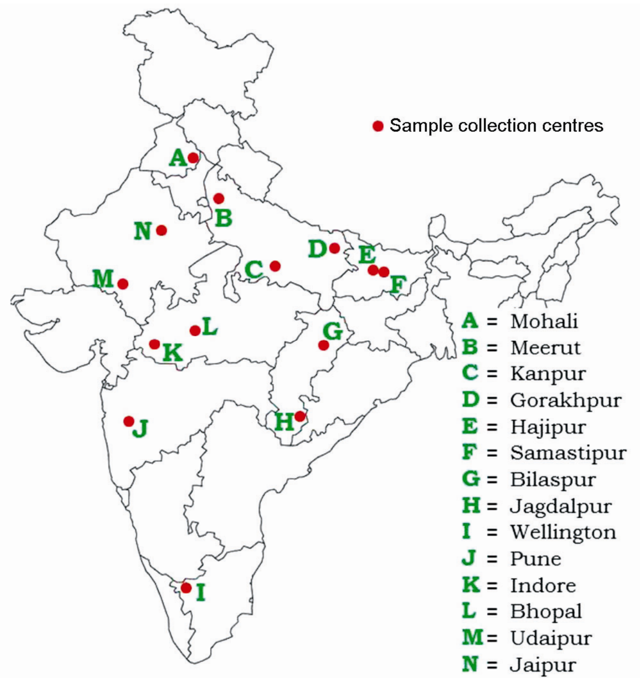

Figure 1. Map of India showing locations from where wheat plant samples were collected. A total of 14 collection centres are shown.

Table 1. Pathogenicity scale and phenotypes

Pathogenicity scale	Plant mean height* (mean height of three plants in cm ± SD)	Primary (dwarfing) phenotype	Additional phenotype
0	72.6 ± 1.52	Healthy looking plants	–
1	67.7 ± 2.08	Slight dwarfing	–
2	65.5 ± 2.56	Slight dwarfing	Yellowing of leaves
3	65.6 ± 1.52	Slight dwarfing	Leaf rust
4	63.5 ± 2.08	Slight dwarfing	Leaf rust and stripe rust
5	48.6 ± 1.52	Moderate dwarfing	–
6	48.1 ± 2.08	Moderate dwarfing	Yellowing of leaves
7	46.6 ± 3.51	Moderate dwarfing	Leaf rust and stripe rust
8	24.6 ± 1.73	Extreme dwarfing	Sterile spikes
9	23.9 ± 1.52	Extreme dwarfing	Yellowing of leaves and sterile spikes

*Height of a representative cultivar (C306) at different disease scales.
–, No additional phenotype.

Table 2. Geographical coordinates of sample collection sites and prevalence of *wheat dwarf India virus* disease complex in the wheat fields

Location	Geographical coordinates	No. of symptomatic samples tested	No. of positive samples			No. of units* tested	Average no. per unit area*			
			WDIV	Alpha	Beta		No. of plants	No. of plants tested	Positive samples	Prevalence of infected plants (%)
Mohali	30°47′N, 76°41′E	317	263	257	245	5	261 ± 3	63 ± 1	52 ± 1	19.9
Meerut	28°58′N, 77°42′E	67	59	56	45	3	240 ± 5	22 ± 1	20 ± 1	8.3
Kanpur	26°45′N, 80°31′E	30	23	21	17	1	246	30	23	9.3
Gorakhpur	29°45′N, 75°66′E	24	18	17	15	1	275	24	18	6.5
Samastipur	25°80′N, 85°67′E	40	36	35	29	2	253 ± 4	20	18 ± 1	7.1
Hajipur	25°68′N, 85°22′E	20	17	13	15	1	270	20	17	6.2
Bilaspur	22°4′N, 82°9′E	45	33	33	32	3	244 ± 6	15	11 ± 1	4.5
Jagdalpur	20°37′N, 81°35′E	40	28	24	21	2	236 ± 8	20	14 ± 2	5.9
Wellington	11°22′N, 76°47′E	78	71	69	55	3	233 ± 5	26 ± 1	24 ± 1	10.3
Pune	18°6′N, 74°18′E	75	69	61	59	3	237 ± 7	25	23 ± 1	9.7
Indore	22°43′N, 75°49′E	60	54	50	51	3	242 ± 6	20	18 ± 1	7.4
Bhopal	23°12′N, 77°27′E	20	15	10	9	1	247	20	15	6.1
Udaipur	24°34′N, 73°38′E	77	55	46	49	3	251 ± 4	26 ± 1	18 ± 1	7.1
Jaipur	26°5′N, 75°47′E	70	50	48	47	3	245 ± 6	23 ± 1	17 ± 1	6.9

One unit means an area of 10 sq. ft each.
Prevalence, Positive samples in a unit area × 100 ÷ no. of plants in a unit area.

JQ361910 and JQ361911) reported earlier from wheat[1]. It exhibited typical mastrevirus genome organization. The betasatellites detected from the samples exhibited an identity of 98% to Ageratum yellow leaf curl betasatellite (AYLCB) reported earlier from wheat[2]. Nucleotide sequence analysis of alphasatellites from different wheat samples revealed that one alphasatellite was close to Cotton leaf curl Multan alphasatellite (CLCuMA) with identity ranging from 95% to 98%. The other molecule resembled Guar leaf curl alphasatellite (GLCuA) with an identity of 93%. CLCuMA was detected in wheat samples collected from all the 14 centres, whereas GLCuA was found only at two centres, Mohali and Wellington.

The prevalence of *WDIV* and the associated satellites in field samples of wheat plants varied at different locations, being the lowest at 4.5% and highest at 19.9% (Table 2). Both the alphasatellite and betasatellite were found at all the locations (Table 2) in *WDIV*-positive samples, but not in the samples that tested negative for *WDIV*.

The disease severity scale was recorded for each cultivar at each location. The cultivars, WL-711, K-65, C-306 and WH-291 were most susceptible among the studied wheat genotypes (Table 3).

The diseased samples, categorized into different disease scales, showed the presence of *WDIV* and associated satellites. The number of diseased plants across the collection centres was largely at scales 1–4, followed by plants at scales 5–7 (Table 4). A few diseased plants were found at scales 8 and 9 (Table 4).

The number of tillers formed was less in the disease scales 8 and 9. The length of the ear was also reduced in these scales (Table 4). Significant variations were observed in thousand grain weight – measured as described by Singh *et al.*[10] – at different disease scales. Thousand grain

Table 3. Varietal effect on disease symptom expression across the country

Variety/cultivar	Pathogenicity scale at different locations									
	Scale 9	Scale 8	Scale 7	Scale 6	Scale 5	Scale 4	Scale 3	Scale 2	Scale 1	Scale 0
WL-711	1, 9, 11, 13, 14	1, 9, 11, 13	1–3, 5, 7–11, 13, 14	–	–	1, 5, 9, 13	1, 5, 7–11, 13, 14	–	2, 3, 5, 7	1–3, 5, 7–11, 13, 14
PBW-343	–	–	1–3, 5, 9, 11, 13, 14	–	4, 12	1, 5, 9, 13, 14	1, 5, 9, 11, 14	4, 6	4, 6, 12	1–6, 9, 11–14
K-65	1, 9, 14	1, 9, 14	2, 3, 7, 8, 10, 13	–	–	2, 3, 7, 8, 10	2, 3, 10, 13	–	2, 3, 7, 8	1–10, 13, 14
C-306	9	1, 9	2, 3, 5, 7–11, 14	4, 6, 12, 13	4, 6, 12, 13	2, 3, 5, 7–11	2, 3, 5, 9, 14	4, 6, 12	4, 6, 12	1–14
Sonalika	–	–	–	–	–	–	–	7, 9, 11, 14	1–3, 5–7, 9	1–7, 9, 11, 14
LOK-1	–	–	–	1–3, 5, 7–11, 13, 14	1, 5, 9, 13, 14	–	–	4, 12	4, 6, 12	1–14
HD-2329	–	–	1, 5, 9, 11, 13, 14	7, 8, 10	7, 8, 10	1, 5, 9, 11, 14	1, 5, 9, 13, 14	–	7, 8	1, 5, 7–11, 13, 14
HD-2781	–	–	–	3, 9, 14	1–3, 9, 14	–	–	–	1, 9, 13	1–3, 9, 13, 14
HD-3016	–	–	–	1, 9	1, 2, 9, 14	–	–	–	1, 2, 9	1, 2, 9, 14
WH-542	–	–	1–3, 5, 9, 11, 13, 14	–	–	1, 5, 9, 11, 13	1–3, 5, 9, 14	–	1, 3, 5, 9	1–3, 5, 9, 11, 13, 14
NI-5439	–	–	1–3, 5, 7, 9, 11, 14	–	–	1, 5, 9, 11, 14	3, 5, 7, 9	–	2, 3, 5, 7	1–3, 5, 7, 9, 11, 14
HI-1568	–	–	1, 2, 7–10, 14	–	–	1, 2, 7, 14	1, 2, 9, 14	–	1, 2, 7, 10	1, 2, 7–10, 14
NIAW-917	–	–	1–3, 5, 7–9, 11, 14	–	–	1, 5, 9, 11, 14	5, 7–9, 11, 14	–	1, 2, 5, 11	1–3, 5, 7–9, 11, 14
RAJ-3765	–	–	–	1, 9, 11, 14	9, 11, 14	–	–	–	1, 9, 11	1, 9, 11, 14
WH-291	1, 9	1, 9	1–3, 5, 7–11, 14	–	–	1–3, 5, 7–11, 14	1–3, 5, 7–11, 14	–	1, 2, 5, 7	1–3, 5, 7–11, 14
GW-366	–	–	–	1–3, 9, 14	1–3, 9, 14	–	–	1–3, 14	1–3, 5, 7, 14	1–3, 5, 7, 9, 14
GW-391	–	–	–	1–3, 9	1, 3, 9	–	–	1–3	1, 2, 9	1–3, 9
GW-322	–	–	–	3, 9	1–3	–	–	1–3	1–3	1–3, 9
HD-2985	–	–	–	1–3, 9–11, 14	3, 9, 10, 14	–	–	1, 2, 11, 14	1, 11	1–3, 9–11, 14
HD-2932	–	–	–	1–3, 9, 14	1–3, 9, 14	–	–	1–3, 9, 14	1–3, 9, 14	1–3, 9, 14
K-8027	–	–	1–3, 9, 14	–	–	3, 14	9, 14	1–3, 9, 14	9, 14	1–3, 9, 14
PBW-299	–	–	–	1–3, 9, 14	9, 14	–	–	–	1, 3	1–3, 9, 14
PBW-550	–	–	–	1–3, 5, 7, 9	1, 9, 13, 14	–	–	7, 9, 13, 14	1, 2, 5	1–3, 5, 7, 9, 13, 14
DBW-17	–	–	–	1–3, 9, 14	1–3, 9, 14	–	–	1, 2, 9, 14	1, 2, 9, 14	1–3, 9, 14
UP-2425	–	–	–	1–3, 9, 14	1, 2, 9	–	–	1, 2	1, 9	1–3, 9, 14
HD-3007	–	–	1–3, 9, 14	–	–	1, 9	14	–	1, 2, 9	1–3, 9, 14

1, Mohali; 2, Meerut; 3, Kanpur; 4, Gorakhpur; 5, Samastipur; 6, Hajipur; 7, Bilaspur; 8, Jagdalpur; 9, Wellington; 10, Pune; 11, Indore; 12, Bhopal; 13, Udaipur; 14, Jaipur; –, Nil.

Table 4. Correlation of pathogenicity scales with productivity traits

Pathogenicity scale	No. of plants collected	No. of virus-positive plants	Percentage of positive plants	Average of 10 independent observations: No. of tillers/ plant	No. of ears/ plant	Length of ear (cm)	Total grain weight/ plant (g)	Thousand grain weight (g)
8–9	15	14	93.3	5–6	5–6	5–8	No grain	No grain
5–7	406	349	85.9	8–15	8–15	7–10	8–15	35 ± 4
1–4	542	426	78.5	5–15	5–15	7–12	12–37	41 ± 4
0	42	2	4.7	5–16	5–16	8–14	13–39	44 ± 5

weight at scale 0 was 44 g (± 5 g) that gradually decreased to 35 ± 4 g at higher disease scale (Table 4). Grain formation was nil in the spikes at scales 8 and 9 (Table 4).

Our survey documented the incidence and prevalence of a previously unreported type of virus, i.e. a mastrevirus with satellites. Somewhat unexpectedly, the mastrevirus disease complex, *WDIV* and the satellites, were present in wheat fields in different ecoclimatic zones in India and showed the presence of both the satellites at all the locations. Prevalence of *WDIV* disease complex was as high as 19.9% at Mohali. It contrast to what has been reported since the discovery of mastreviruses, all *WDIV*-infected plants collected from widely separated geographical locations across the country contained both the alphasatellite and betasatellite. The virus has been missed by earlier wheat researchers in India, and the mastreviruses from other countries have not been reported to contain the satellite DNAs.

The satellites (GLCuA, CLCuMA and AYLCB) identified in the present study, have recently been reported by us to be associated with *WDIV*[2,3]. These were characterized to enhance symptom development. In laboratory infections, we reported that each of the satellites added incrementally to symptom expression and virus accumulation in the infected plants[2]. However, under natural infection in field, both the satellites were found associated with the diseased plants at all disease scales in all the cultivars tested, and at all the locations. A substantial varietal effect was recorded on disease severity (scale 1–9), suggesting the significance of host–pathogen interactions. At the same time, a given cultivar exhibited different disease scales at different locations, suggesting the effect of environment on varietal susceptibility. Among the 26 cultivars scored at different field locations, Sonalika was the most resistant cultivar and WL-711 was most sensitive to *WDIV*. The presence of different disease scales in a given cultivar at a given location is possibly because of the effect of plant age and microconditions at the time of infection. However, the detection of *WDIV* in two plants of cultivar Sonalika at scale 0 suggests that *WDIV* infection to these plants may have been initiated at a late stage of growth. Also, Sonalika has been reported to show mild symptoms in laboratory inoculation by *WDIV* and the satellites[2].

The highest number of plants was found at disease scale 1–4, followed by 5–7. The number of infected plants was few at disease scale 8 and 9. Hence, most of the wheat cultivars investigated during this study may be considered as resistant or moderately susceptible. The incidence and prevalence levels of *WDIV* disease complex on the basis of observed disease symptoms were established by PCR-based amplification and sequencing. The disease incidence and prevalence of *WDIV* was highest at Mohali and lowest at Bilaspur. Our study suggests that a number of factors, including environmental conditions, plant developmental stage and varietal type may determine the prevalence of *WDIV* disease complex in wheat besides the prevalence of the insect vector. The reduction in the number of tillers, length of ear and grain weight per plant in the diseased plants suggests the potential effect of viral infection on yield of wheat crop.

Wide prevalence of *WDIV* disease complex in India could be a potential threat to wheat production and therefore warrants studies to limit its spread, and also find alternative hosts, vectors and strategies for resistance. At present, the virus does not appear to cause economic loss to wheat yield. However, cultivar-specific field data in different regions of India need to be collected for detailed assessment. The association of the satellites with a mastrevirus opens new possibilities in developing novel vectors for genomic studies in wheat and examining the effect of the satellites on host range and pathogenesis.

1. Kumar, J., Singh, S. P., Kumar, J. and Tuli, R., A novel mastrevirus infecting wheat in India. *Arch. Virol.*, 2012, **157**, 2031–2034.
2. Kumar, J., Kumar, J., Singh, S. P. and Tuli, R., Association of satellites with a mastrevirus in natural infection: complexity of *Wheat dwarf India virus* disease. *J. Virol.*, 2014, **88**, 7093–7104.
3. Kumar, J., Kumar, J., Singh, S. P. and Tuli, R., *β*C1 is a pathogenicity determinant: not only for begomoviruses but also for a mastrevirus. *Arch. Virol.*, 2014, **159**, 3071–3076.
4. Tóbiás, I. *et al.*, Comparison of the nucleotide sequences of wheat dwarf virus (WDV) isolates from Hungary and Ukraine. *Pol. J. Microbiol.*, 2011, **60**, 125–131.
5. Mesterházy, Á., Gáborjányi, R., Papp, M. and Fónad, P., Multiple virus infection of wheat in South Hungary. *Cereal Res. Commun.*, 2002, **30**, 329–334.
6. Schubert, J., Habekuß, A., Kazmaier, K. and Jeske, H., Surveying cereal-infecting geminiviruses in Germany – diagnostics and direct sequencing using rolling circle amplification. *Virus Res.*, 2007, **127**, 61–70.
7. Ramsell, J. N. E., Lemmetty, A., Jonasson, J., Andersson, A., Sigvald, R. and Kvarnheden, A., Sequence analyses of *Wheat*

dwarf virus isolates from different hosts reveal low genetic diversity within the wheat strain. *Plant Pathol.*, 2008, **57**, 834–841.
8. Zhang, X., Zhou, G. and Wang, X., Detection of wheat dwarf virus (WDV) in wheat and vector leafhopper (*Psammotettix alienus* Dahlb.) by real-time PCR. *J. Virol. Methods*, 2010, **169**, 416–419.
9. Kumar, J., Kumar, A., Roy, J. K., Tuli, R. and Khan, J. A., Identification and molecular characterization of begomovirus and associated satellite DNA molecules infecting *Cyamopsis tetragonoloba*. *Virus Genes*, 2010, **41**, 118–125.
10. Singh, S. P. *et al.*, Pattern of iron distribution in maternal and filial tissues in wheat grains with contrasting levels of iron. *J. Exp. Bot.*, 2013, **64**, 3249–3260.

ACKNOWLEDGEMENTS. The authors are grateful to the Department of Biotechnology, Government of India for supporting the present work at National Agri-Food Biotechnology Institute, Mohali, India; to the Council of Scientific and Industrial Research for Fellowships to Jitendra Kumar and Jitesh Kumar, and to the Department of Science and Technology, Government of India for the JC Bose Fellowship to RT; to scientists and head of the research centres (Table S1, see Supplementary Information online) and also to farmers for allowing us to collect wheat samples.

Received 18 October 2013; revised accepted 30 September 2014

Magnetic fabric studies of sandstone from Jhuran Formation (Kimmeridgian–Tithonian) of Jara dome, Kachchh Basin, northwest India

V. Periasamy and M. Venkateshwarlu*

CSIR-National Geophysical Research Institute, Uppal Road, Hyderabad 500 007, India

Low-field anisotropy of magnetic susceptibility (AMS) study was performed on the clastic sandstones of the Jhuran Formation from the Jara dome in the Kachchh basin. The AMS results consistent with petrographic analysis indicate primary deposition fabric for Arkose, sub-litharenite, wacke and quartz arenite sandstones of the Jhuran Formation. Isothermal remanent magnetization and thermal demagnetization curves indicate that magnetite, titano-magnetite and hematite are the chief magnetic minerals contributing to the AMS. The distribution of K_1, K_2 and K_3 axes in the stereographic projections suggest depositional fabric development for arkose, sub-litharenite and wacke, whereas dispersed K_3 axes for quartz arenite are inferred to be due to low strain activity. The shape factors T, q confirm the oblate-shaped ellipsoid and horizontal fabric respectively, for all samples. The reconstructed palaeoflow directions for arkose and sub-litharenite are NW–SE and for wacke and quartz arenite are NE–SW based on K_1 AMS axis.

Keywords: AMS, magnetic fabric, Kachchh basin, palaeoflow directions.

IN clastic sedimentary rocks, magnetic fabric is produced during physical transportation and deposition of magnetic particles. Studies of the magnetic fabric provide information concerning palaeoflow directions, environment of deposition, influence of tectonism and weak deformation of rock units[1–3]. The low-field anisotropy of magnetic susceptibility (AMS) is a widely used technique to determine the magnetic fabric and palaeoflow direction of the sediments and sedimentary rocks, particularly sandstone. Generally the shape of the magnetic susceptibility ellipsoids provides insight into the mode of deposition, i.e. in still water, the minimum susceptibility axes of the grains are clustered on the pole, while the maximum and intermediate axes disperse uniformly on the bedding plane. Whereas the flowing water current results in the alignment of susceptibility axes which lie in different directions[4–8].

This communication presents AMS results of sandstone of the Upper Jurassic (Kimmeridgian to Tithonian) Jhuran Formation exposed in Jara dome in the Kachchh sedimentary basin.

The Kachchh basin is located in western India (Figure 1). Formation of the basin is linked to the break-up between eastern and western Gondwanaland during Late Triassic/Early Jurassic period[9–11]. The rift basin contains several intra-basinal strike faults such as the Island Belt Fault (IBF), the Banni Fault (BF), the Kachchh Mainland Fault (KMF), the Katrol Hill Fault (KHF) and the South Wagad Fault (SWF). A first-order meridional (NNE–SSW) high is found across the middle of the basin[12].

The basin consists of 2000–3000 m thick Mesozoic sediments ranging in age from Lower Jurassic to Lower Cretaceous, 600 m of Tertiary sediments and a thin sheet of Quaternary sediments. The rock outcrops are better exposed in the uplifted regions of the basin, such as Kachchh Mainland, Pachham Island, Khadir Island, Bela Island, Chorar Island and Wagad uplifts. Lower Jurassic to Lower Cretaceous are well preserved in the Kachchh Mainland. The stratigraphic succession of Kachchh Mainland is divided into four formations, namely Jhurio (Bathonian to Callovian), Jumara (Callovian to Oxfordian), Jhuran (Kimmeridgian to Lower Cretaceous) and Bhuj (pre-Aptian to Santonian (?)) Formations in ascending stratigraphic order[13], are best exposed in a series of domes at Habo, Jhura, Keera, Nara, Jumara and Jara hills (Figure 1). The lithological sequence of these formations consists of clastic sandstone, siltstone, shale and limestone with distinct demarcation boundary, deposited in marine to fluviodeltaic conditions.

*For correspondence. (e-mail: mamila_v@rediffmail.com)